Autophagy Inhibition with Monensin Enhances Cell Cycle Arrest and Apoptosis Induced by mTOR or Epidermal Growth Factor Receptor Inhibitors in Lung Cancer Cells

Hyeong Sim Choi, M.S., Eun-Hui Jeong, M.S., Tae-Gul Lee, M.S., Seo Yun Kim, M.D., Hye-Ryoun Kim, M.D. and Cheol Hyeon Kim, M.D.
Division of Pulmonology, Department of Internal Medicine, Korea Cancer Center Hospital, Seoul, Korea

Background: In cancer cells, autophagy is generally induced as a pro-survival mechanism in response to treatment-associated genotoxic and metabolic stress. Thus, concurrent autophagy inhibition can be expected to have a synergistic effect with chemotherapy on cancer cell death. Monensin, a polyether antibiotic, is known as an autophagy inhibitor, which interferes with the fusion of autophagosome and lysosome. There have been a few reports of its effect in combination with anticancer drugs. We performed this study to investigate whether erlotinib, an epidermal growth factor receptor inhibitor, or rapamycin, an mammalian target of rapamycin (mTOR) inhibitor, is effective in combination therapy with monensin in non-small cell lung cancer cells.
Methods: NCI-H1299 cells were treated with rapamycin or erlotinib, with or without monensin pretreatment, and then subjected to growth inhibition assay, apoptosis analysis by flow cytometry, and cell cycle analysis on the basis of the DNA contents histogram. Finally, a Western blot analysis was done to examine the changes of proteins related to apoptosis and cell cycle control.
Results: Monensin synergistically increases growth inhibition and apoptosis induced by rapamycin or erlotinib. The number of cells in the sub-G_1 phase increases noticeably after the combination treatment. Increase of proapoptotic proteins, including bax, cleaved caspase 3, and cleaved poly(ADP-ribose) polymerase, and decrease of anti-apoptotic proteins, bcl-2 and bcl-xL, are augmented by the combination treatment with monensin. The promoters of cell cycle progression, notch3 and skp2, decrease and p21, a cyclin-dependent kinase inhibitor, accumulates within the cell during this process.
Conclusion: Our findings suggest that concurrent autophagy inhibition could have a role in lung cancer treatment.

Keywords: Autophagy; Apoptosis; Cell Cycle; Monensin; Epidermal Growth Factor Receptor-Neu Receptor; TOR Serine-Threonine Kinases

Introduction

Autophagy is a defense mechanism to protect cells from multiple stresses such as nutrient starvation, hypoxia, pathogen infection, and radiation[1]. During the initial stages of the autophagic process, long-lived cellular proteins and organelles are sequestered and engulfed by intracellular double-membrane-bound structures called autophagosomes (early autophagic vesicles)[2]. Autophagosomes mature by fusing with lysosomes to form autolysosomes (late autophagic vesicles), in which the sequestered proteins and organelles are digested by lysosomal hydrolases and recycled to sustain cellular metabolism[3]. In addition, autophagy is observed in cancer cells upon treatment with a wide spectrum of cytotoxic and targeted chemotherapeutic agents[3-5]. Thus, concurrent autophagy inhibition can be expected to have a synergistic effect with chemotherapy on cancer cell death[4].

Monensin, a polyether antibiotic, is known as an autophagy inhibitor, which interferes with the fusion of autophagosome and lysosome and thus blocks the autophagic process at its final step[6]. Used alone, its cytotoxic effect is negligible and there have been few reports of its effect in combination with standard anticancer drugs[5,6].

The epidermal growth factor receptor (EGFR) is a member of the receptor tyrosine kinase family, which is important in cancer cell growth, proliferation, invasion, and metastasis[7]. It is frequently deregulated in non-small cell lung cancer (NSCLC)[8]. Tyrosine kinase inhibitors such as gefitinib and erlotinib have been developed for the treatment of NSCLC, through inhibition of the tyrosine kinase activity of EGFR[9]. Gefitinib and erlotinib are effective in NSCLC cells harboring activating *EGFR* mutations, but not in cells with wild type *EGFR*[10,11].

The phosphoinositide 3-kinase (PI3K)/Akt/mammalian target of rapamycin (mTOR) pathway is activated in many cancers, including NSCLC[12,13]. This signaling pathway plays an important role in cell growth, cell proliferation, angiogenesis, and protein synthesis[14]. Inhibitors of mTOR, including rapamycin, have demonstrated efficacy in vitro and are now being tested in early-phase clinical trials in NSCLC[13].

In this study, we investigated whether erlotinib, an EGFR inhibitor, or rapamycin, an mTOR inhibitor, is effective in combination therapy with monensin in NSCLC cells. We also explored the mechanisms of the combination effect, and demonstrated that the inhibition of autophagy with monensin enhances rapamycin- and erlotinib-induced apoptotic cell death and cell cycle arrest.

Materials and Methods

1. Cell cultures

NCI-H1299 cells, which are derived from NSCLC and lack

EGFR mutations, were purchased from the American Type Culture Collection (Rockville, MD, USA). NCI-H1299 cells were maintained as monolayer cultures in RPMI 1640 medium supplemented with 10% fetal bovine serum, 1% penicillin-streptomycin, and 1% sodium pyruvate, at $37^{o}C$ in a humidified incubator under 5% CO_2 gas. All cell culture materials were obtained from Welgen (Daegu, Korea).

2. Reagents

Acridine orange (AO), dimethyl sulfoxide (DMSO), propidium iodide (PI), 3-(4,5-dimethyl thiazol-2-yl)-2,5-diphenyl tetrazolium bromide (MTT) solution, and anti-β-actin antibody were purchased from Sigma (St. Louis, MO, USA). Monensin, rapamycin, and erlotinib were purchased from Selleck (Houston, TX, USA). The Annexin V-FITC kit and anti-p21 antibody were obtained from BD Biosciences (San Jose, CA, USA). Antibodies against phospho-p70S6K, LC3, caspase-3, cleaved-caspase 3, poly(ADP-ribose) polymerase (PARP), bcl-2, and notch3 were purchased from Cell Signaling Technology (Beverly, MA, USA). Antibodies against bax, bcl-xl, skp2, and p27 and horseradish peroxidase (HRP)-conjugated secondary antibodies were obtained from Santa Cruz Biotechnology (Santa Cruz, CA, USA). The enhanced chemiluminescence (ECL) Western blotting detection system was supplied by Amersham Biosciences (Piscataway, NJ, USA).

3. Treatments

NCI-H1299 cells were seeded in a 96-well plate (1.2×10^3 cells/50 μL) and incubated at $37^{o}C$. The next day, cells were pre-treated with 50 nM monensin for 4 hours, followed by treatment with varying concentrations of rapamycin or erlotinib for 48 hours, after which further analysis was performed. Rapamycin (20 mM), erlotinib (40 mM), and monensin (1 mM) were dissolved in DMSO. As a control, equal volumes of DMSO (0.05%) were added to untreated cells.

4. Analysis of cell viability

Inhibition of cell proliferation was determined by a MTT assay. MTT solution was added to cells in 96-well plates to a final concentration of 0.5 mg/mL, and cells were incubated at $37^{o}C$ for 4 hours. After removing the culture media, 50 μL of DMSO was added, and the optical density of each well was read at 590 nm.

5. Quantification of acidic vesicular organelles (AVOs) with AO staining

Cells were seeded in 60 mm dishes and treated with rapamycin or erlotinib with or without pretreatment with 50 nM monensin for 4 hours. 48 hours after incubation, AO staining

was performed; briefly, the treated cells were stained with AO (1 μg/mL in serum-free RPMI 1640 media) in the dark at 37°C for 15 minutes, and then washed with serum-free RPMI 1640 media. Images of AO staining were visualized immediately using a Leica confocal laser scanning microscope (Wetzlar, Germany).

6. Annexin V-FITC assay by flow cytometry

After incubation with each agent, cells were washed with phosphate buffered saline (PBS), trypsinized, collected in a 15 mL conical tube, and pelleted by centrifugation (1,200 rpm) for 10 minutes at room temperature. The pellets were washed twice with PBS, and then resuspended in annexin V binding buffer (150 mM NaCl, 18 mM $CaCl_2$, 10 nM HEPES, 5 mM KCl, 1 mM $MgCl_2$). Fifteen minutes after incubation with annexin V (1 g/mL) in the dark, the cells were analyzed using a FACS-Canto II flow cytometer (BD, San Jose, CA, USA).

7. DNA content analysis by flow cytometry

After incubation, cells were washed with ice-cold PBS, trypsinized, collected in a 15 mL conical tube, and pelleted by centrifugation (1,200 rpm) for 10 minutes at 4°C. The pellets were washed twice with ice-cold PBS, fixed in 70% ethanol, washed in PBS, resuspended in 300 μL of PBS containing 50 μg/mL PI and 50 μg/mL RNase A, and incubated in the dark for 15 minutes at room temperature. The DNA content of each cell nucleus was determined by flow cytometry.

8. Western blot analysis

Thirty micrograms of protein were resolved by 10% sodium dodecyl sulfate polyacrylamide gel electrophoresis and transferred to nitrocellulose membranes. The membranes were blocked with 5% skim milk-PBS-0.1% Tween 20 for an hour at room temperature before being incubated overnight with primary antibodies diluted 1:1,000 in 5% skim milk–PBS-0.1% Tween 20. The membranes were then washed three times in 1× PBS–0.1% Tween 20 and incubated with HRP-conjugated secondary antibodies diluted 1:2,000 in 5% skim milk–PBS–0.1% Tween 20 for an hour. After successive washes, the membranes were developed using an ECL kit.

9. Analysis of combination effects

For the statistical analysis of the synergistic effect of drug co-administration on MTT analysis, combination indexes (CI) were calculated using CalcuSyn software version 2.1 (Biosoft, Cambridge, UK). CI<0.7 indicates synergistic effects (the smaller the value, the stronger the synergism); CI=1 indicates additive effects; and CI values>1 suggest antagonistic effects.

10. Statistical analysis

All cell viability experiments were repeated three times. Cell viability data are presented as mean±standard deviation percentage of control of three different experiments. Mann-Whitney U-test was used for comparisons and p<0.05 was considered as statistically significant.

Results

1. Growth inhibition induced by rapamycin or erlotinib is enhanced by combination treatment with monensin in NCI-H1299 cells

We examined the cell growth inhibition of rapamycin or erlotinib when each drug was combined with monensin, an autophagy inhibitor. NCI-H1299 cells were pretreated with monensin (50 nM) for 4 hours and then treated with various concentrations (0–20 μM) of rapamycin or erlotinib for 48 hours. Figure 1A shows that both rapamycin- and erlotinib-induced morphological change and cell growth inhibition, observed by light microscopy, are increased by adding treatment with monensin. Cell viability was also measured using the MTT assay (Figure 1B). Treatment with each drug alone causes a slight decrease in cell proliferation; by contrast, this decrease is significantly enhanced when cells are treated in combination with monensin. To assess whether this combination effect is synergistic or additive, we calculated the CI at each concentration (2.5–20 μM). As shown in Figure 1C, the CI values of all combinations tested are below 0.7, indicating that the agents act synergistically when used as combination treatments in NCI-H1299 cells.

2. Autophagy inhibition by monensin enhances apoptosis induced by rapamycin or erlotinib in NCI-H1299 cells

We investigated whether the observed changes in growth inhibition induced by monensin were due to enhanced apoptosis. First, we performed AO staining to detect the AVOs formed during the process of autophagy (Figure 2A). Both rapamycin- and erlotinib-treated cells show plentiful orange staining, but cotreatment with monensin (50 nM), which inhibits fusion of autophagosomes with lysosomes, effectively suppresses the development of AVOs in NCI-H1299 cells. Then we performed Annexin V-FITC assays by flow cytometry. As shown in Figure 2B, monensin cotreatment increases annexin V-positive apoptotic cells to about 20% compared with treatment using rapamycin or erlotinib alone. We also analyzed the sub-G_1 cell population, characteristic of apoptosis, by flow cytometry with PI staining (Figure 2C). The sub-G_1 cell population increases significantly when monensin is used

A

Control   Rapa 10 μM   Erl 10 μM   Mon 50 nM   Rapa 10 μM+ Mon 50 nM   Erl 10 μM+ Mon 50 nM
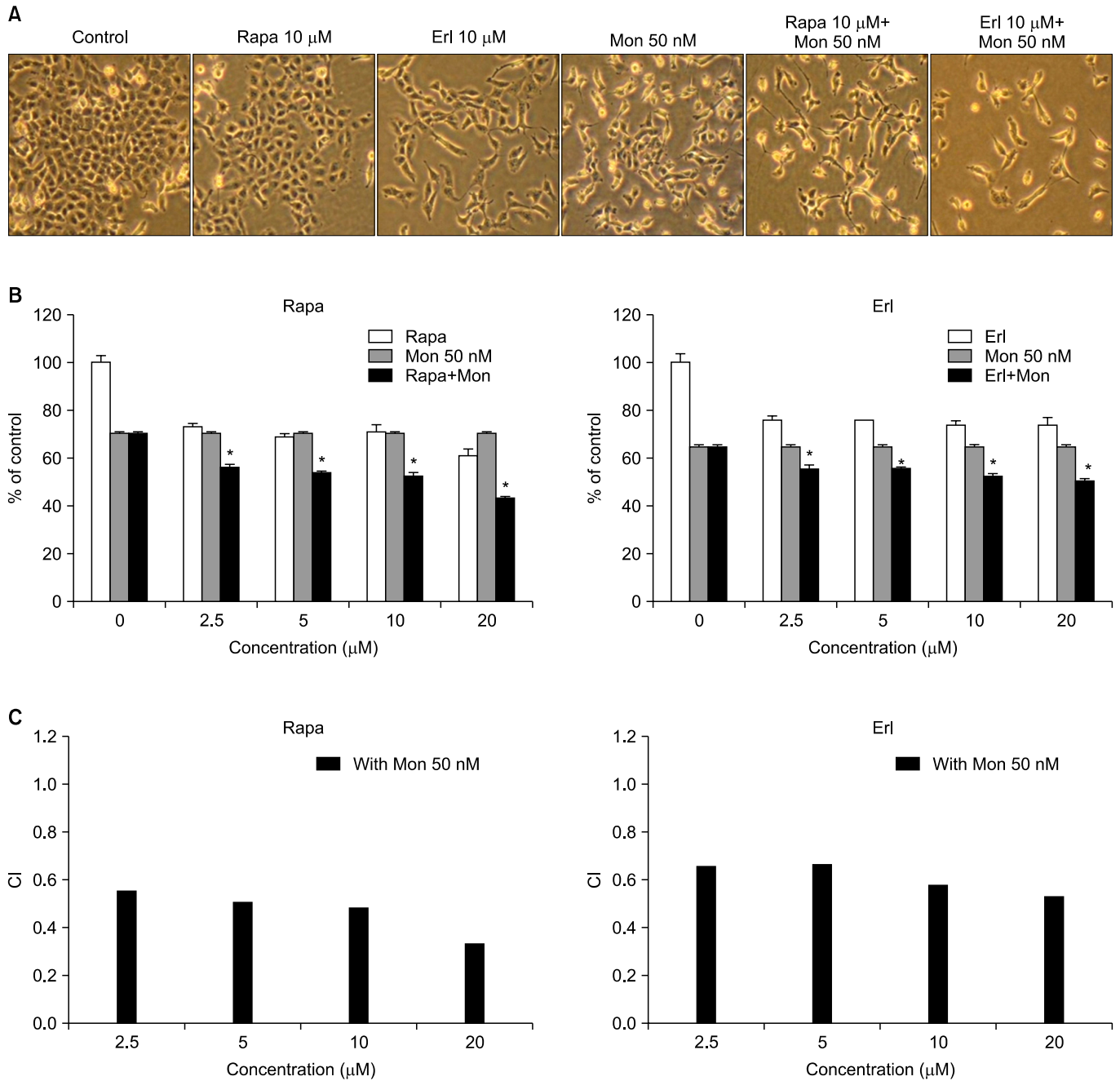
B

C

Figure 1. Enhancement of growth inhibition by combination treatment with monensin and rapamycin or erlotinib in NCI-H1299 cells. NCI-H1299 cells were pretreated with 50 nM monensin for 4 hours before treatment with 10 μM of rapamycin or erlotinib for 48 hours. (A) Morphology of cells was observed by optical microscopy. Monensin accelerates morphologic changes induced by rapamycin or erlotinib. (B) Cellular growth inhibition was analyzed by MTT assay. Monensin increases the growth inhibition induced by rapamycin or erlotinib. The data shown are representative of three independent experiments with similar results; error bars are mean±standard deviation. Mann-Whitney U-test was used for comparisons. *p<0.01, single versus combination treatment. (C) Effects of monensin in combination with rapamycin or erlotinib on growth inhibition was calculated on the basis of the combination index (CI) of each concentration. CI values<0.7 indicate synergism. Rapa: rapamycin; Erl: erlotinib; Mon: monensin.

in combination treatment with rapamycin (3.62–20.60%) or erlotinib (4.25–22.66%), compared to treatment with either agent alone. These results indicate that the observed combination effect is caused by an increase in apoptosis.
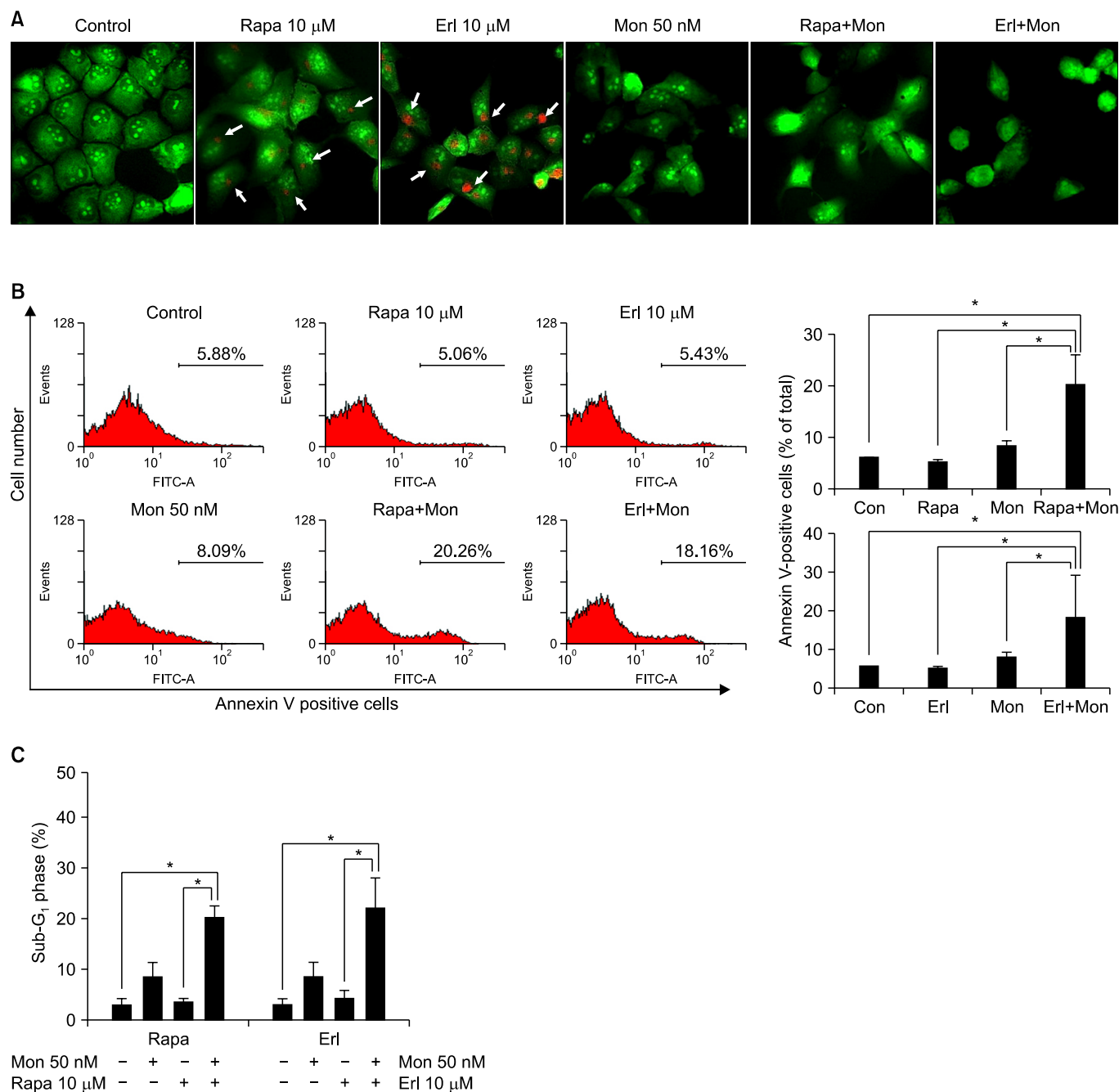
Figure 2. Increased apoptosis by treatment with monensin in combination with rapamycin or erlotinib in NCI-H1299 cells. (A) Inhibition of autophagy was detected by acridine orange staining. NCI-H1299 cells were treated with rapamycin or erlotinib for 48 hours with or without monensin pretreatment, stained with acridine orange (1 μg/mL), and then visualized under a red-filtered confocal microscope. Rapamycin- and erlotinib-induced formation of acidic vesicular organelles (white arrows) is effectively inhibited by monensin treatment. (B) Apoptosis was analyzed by flow cytometry with annexin V staining after each treatment described above. Numbers of annexin V-positive apoptotic cells increase after combination treatment with monensin, compared to treatment with rapamycin or erlotinib alone (left). The percentage of annexin V-positive apoptotic cells was calculated on the basis of the results shown in the histogram (right). The data shown are representative of three independent experiments with similar results; error bars are mean±standard deviation (SD). Mann-Whitney U-test was used for comparisons. *p<0.05, single versus combination. (C) Percentage of cells in the sub-G_1 phase was determined on the basis of the DNA contents histogram from propidium iodide-stained cells. When rapamycin- or erlotinib-treated cells are co-treated with monensin, the number of cells in the sub-G_1 phase noticeably increases. The data shown are representative of three independent experiments with similar results; error bars are mean±SD. Mann-Whitney U-test was used for comparisons. *p<0.01, single versus combination. Con: control; Rapa: rapamycin; Erl: erlotinib; Mon: monensin.
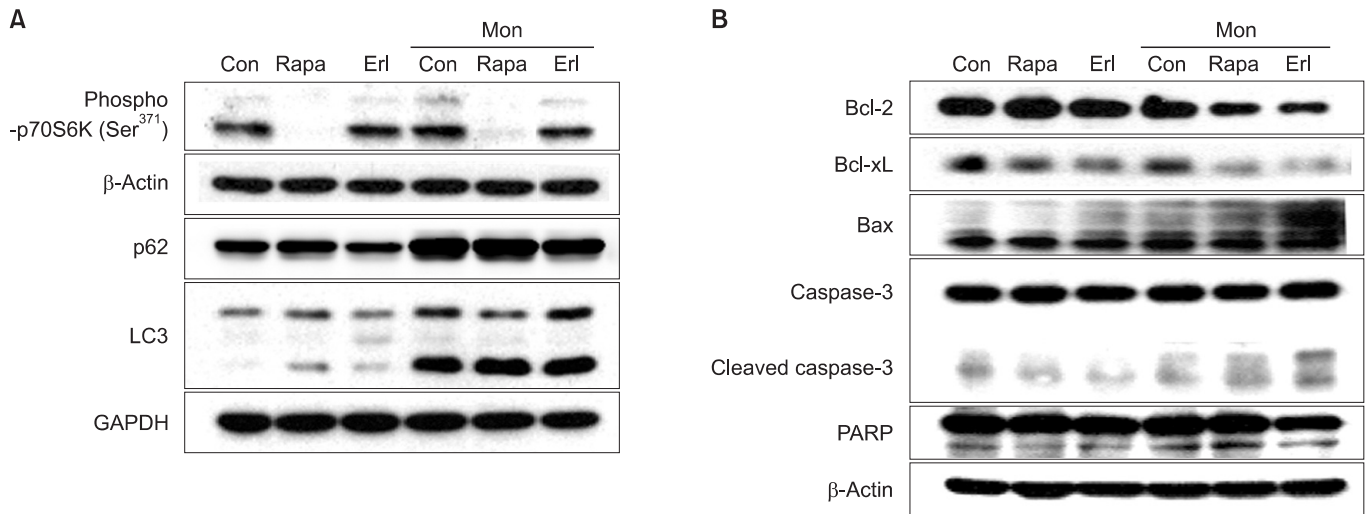
A

B

Figure 3. The combination effect is mediated by apoptotic pathways in NCI-H1299 cells. NCI-H1299 cells were exposed to monensin (50 nM, 4 hours), followed by rapamycin or erlotinib (10 μM, 48 hours), and harvested for western blot analysis. Western blotting was performed with specific antibodies, and β-actin served as a loading control. (A) p-p70S6K expression decreases after treatment with rapamycin or erlotinib. The type II form of LC3 accumulates and degradation of p62 is blocked after treatment with monensin, which blocks fusion of autophagosome and lysosome. (B) After combination treatment, increases of proapoptotic proteins, including bax, cleaved caspase 3, and cleaved poly(ADP-ribose) polymerase (PARP) are enhanced. By contrast, decreases of anti-apoptotic proteins, bcl-2 and bcl-xL, are also augmented. Con: control; Rapa: rapamycin; Erl: erlotinib; Mon: monensin.
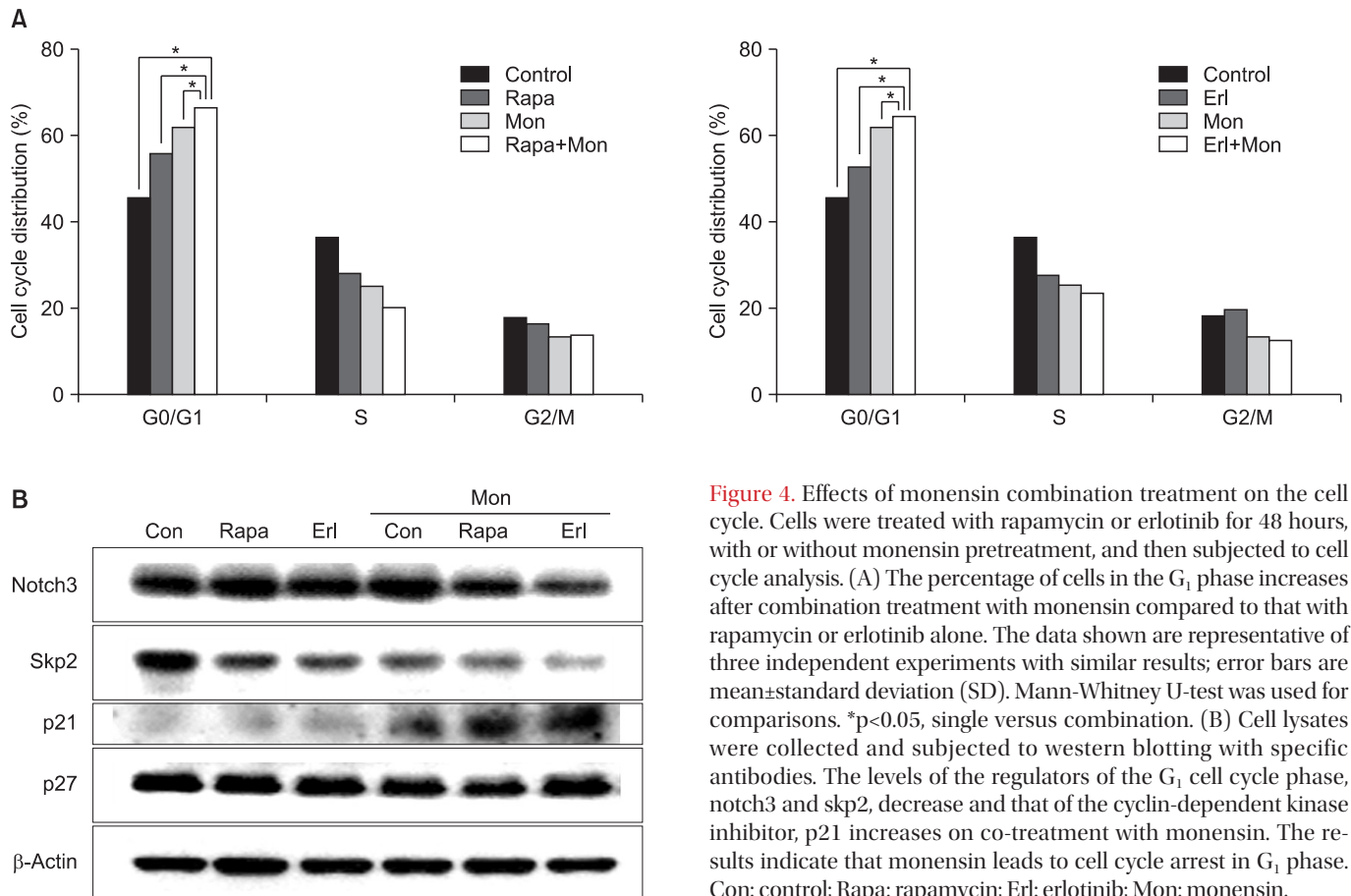
A

B

Figure 4. Effects of monensin combination treatment on the cell cycle. Cells were treated with rapamycin or erlotinib for 48 hours, with or without monensin pretreatment, and then subjected to cell cycle analysis. (A) The percentage of cells in the G_1 phase increases after combination treatment with monensin compared to that with rapamycin or erlotinib alone. The data shown are representative of three independent experiments with similar results; error bars are mean±standard deviation (SD). Mann-Whitney U-test was used for comparisons. *p<0.05, single versus combination. (B) Cell lysates were collected and subjected to western blotting with specific antibodies. The levels of the regulators of the G_1 cell cycle phase, notch3 and skp2, decrease and that of the cyclin-dependent kinase inhibitor, p21 increases on co-treatment with monensin. The results indicate that monensin leads to cell cycle arrest in G_1 phase. Con: control; Rapa: rapamycin; Erl: erlotinib; Mon: monensin.

3. The combination effect of monensin with rapamycin or erlotinib is mediated by apoptotic signaling

We further examined the expression of proteins related to apoptosis during this process in NCI-H1299 cells. First, we confirmed that phosphorylation of p70S6K (a downstream target of mTOR) at Ser[371] is substantially decreased by rapamycin treatment and that type II LC3 (14 kDa), a hallmark of the autophagosome, is remarkably increased and degradation of p62 (an adaptor protein that binds to LC3 and is removed by autophagy) is blocked by monensin treatment, indicating the accumulation of autophagosomes (Figure 3A). When compared to treatment with rapamycin or erlotinib alone, cotreatment with monensin induces increased levels of pro-apoptotic proteins, including Bax, cleaved caspase 3 and cleaved PARP, and decreases the levels of anti-apoptotic proteins, including Bcl-2 and Bcl-xL (Figure 3B).

4. Combination treatment with monensin increases cells arrested in G_1-phase

We also analyzed the effect of monensin treatment on cell cycle progression by flow cytometry with PI staining (Figure 4A). DNA content analysis shows that cotreatment with monensin increases the numbers of cells in the G_1 cycle phase, as compared to treatment with rapamycin or erlotinib alone. Next, we investigated the effect of monensin on cell cycle regulators, including notch3, skp2, p21, and p27 by western blot analysis (Figure 4B). Notch signaling is known to induce skp2 expression and promote reduction of p21 and p27 cyclin-dependent kinase inhibitors. Expression of notch3 and skp2 is decreased after treatment with monensin. In contrast, p21 expression is noticeably increased by monensin treatment. This result is in agreement with the increased G_1 cycle arrest caused by monensin treatment. The levels of p27 are unchanged after each treatment.

Discussion

It is known that the predominant role of autophagy in cancer cells is to confer stress tolerance, which serves to maintain tumor cell survival[1]. Cytotoxic and metabolic stresses, including hypoxia and nutrient deprivation, can activate autophagy for recycling of ATP to maintain cellular biosynthesis and survival[15]. In cancer cells that survive chemotherapy or radiation, activation of autophagy may enable a state of dormancy in residual cancer cells that may contribute to tumor recurrence and progression[4]. Inhibition of autophagy in tumor cells has been shown to enhance the efficacy of anticancer drugs, supporting its role in cytoprotection[16].

Multiple studies have shown that genetic knockdown of autophagy-related genes (Atgs) or pharmacological inhibition of autophagy can effectively enhance tumor cell death induced by diverse anticancer drugs in preclinical models[15,17]. For example, inhibition of autophagy improved responses to alkylating agents in tumor cells[18,19]. In apoptosis-defective leukemic and colon cancer cell lines, inhibition of autophagy was shown to sensitize resistant cells to tumor necrosis factor-related apoptosis-inducing ligand-mediated apoptosis[20]. Furthermore, inhibition of autophagy enhanced apoptosis induction by cetuximab, an antibody against EGFR[21]. However, the effect of autophagy inhibitors on lung cancer chemotherapy is not well documented, and therefore, it was addressed in this study.

Pharmacological inhibitors of autophagy can be broadly classified as early- or late-stage inhibitors of the pathway. Early-stage inhibitors include 3-methyladenine[22], wortmannin[23], and LY294002[24], which target class III PI3K and interfere with its recruitment to membranes. Late-stage inhibitors include chloroquine[25], hydroxychloroquine[26], bafilomycin A1[27], and monensin[6]. Bafilomycin A1 is a specific inhibitor of vacuolar-ATPase, and monensin and chloroquine/hydroxychloroquine are lysosomotropic drugs that prevent the acidification of lysosomes, whose digestive hydrolases depend on low pH. Multiple clinical trials are currently assessing the effects of combined treatments with various anti-cancer drugs plus hydroxychloroquine for patients with various refractory malignancies[28]. Monensin is a monocarboxylic acid ionophore drug isolated from *Streptomyces cinnamonensis*; it can form complexes with metal cations and is able to transport them through cellular and subcellular membranes[6]. Monensin also blocks intracellular protein transport and exhibits antibiotic, antimalarial, and other biological activities[29]. It has an excellent safety record as an additive to beef cattle feed; however, its anticancer effect as an autophagy inhibitor has not been established[30].

In this study, we showed that a nanomolar concentration (50 nM) of monensin can enhance apoptosis induced by rapamycin or erlotinib in NCI-H1299 cells. To the best of our knowledge, this is the first report showing that autophagy inhibition with monensin can enhance the effect of anticancer agents in lung cancer cells. Increased levels of bax, cleaved caspase 3, and cleaved PARP accompany this process. Monensin can also induce accumulation of cells in the G_1 phase by modulating cell cycle regulators. Expression of notch3 and skp2 is decreased but p21 expression increases by monensin treatment. Notch3 and skp2 are positive regulators of cell cycle progression, whereas p21, a cyclin dependent kinase inhibitor, is a negative regulator that causes cell cycle arrest by preventing interaction between cyclins and cyclin-dependent kinases.

Taken together, our data suggest a strategy to enhance the effects of EGFR tyrosine kinase inhibitors and mTOR inhibitors by blocking autophagy, resulting in increased growth inhibition and apoptotic cell death of NSCLC cells.

Acknowledgements

References

1. Marx J. Autophagy: is it cancer's friend or foe? Science 2006; 312:1160-1.
2. Hippert MM, O'Toole PS, Thorburn A. Autophagy in cancer: good, bad, or both? Cancer Res 2006;66:9349-51.
3. Turcotte S, Giaccia AJ. Targeting cancer cells through autophagy for anticancer therapy. Curr Opin Cell Biol 2010;22:246-51.
4. Kondo Y, Kanzawa T, Sawaya R, Kondo S. The role of autophagy in cancer development and response to therapy. Nat Rev Cancer 2005;5:726-34.
5. Boya P, Gonzalez-Polo RA, Casares N, Perfettini JL, Dessen P, Larochette N, et al. Inhibition of macroautophagy triggers apoptosis. Mol Cell Biol 2005;25:1025-40.
6. Huczynski A, Stefanska J, Przybylski P, Brzezinski B, Bartl F. Synthesis and antimicrobial properties of monensin A esters. Bioorg Med Chem Lett 2008;18:2585-9.
7. Hirsch FR, Scagliotti GV, Langer CJ, Varella-Garcia M, Franklin WA. Epidermal growth factor family of receptors in preneoplasia and lung cancer: perspectives for targeted therapies. Lung Cancer 2003;41 Suppl 1:S29-42.
8. Scagliotti GV, Selvaggi G, Novello S, Hirsch FR. The biology of epidermal growth factor receptor in lung cancer. Clin Cancer Res 2004;10(12 Pt 2):4227s-32s.
9. Han W, Pan H, Chen Y, Sun J, Wang Y, Li J, et al. EGFR tyrosine kinase inhibitors activate autophagy as a cytoprotective response in human lung cancer cells. PLoS One 2011;6:e18691.
10. Takezawa K, Okamoto I, Tanizaki J, Kuwata K, Yamaguchi H, Fukuoka M, et al. Enhanced anticancer effect of the combination of BIBW2992 and thymidylate synthase-targeted agents in non-small cell lung cancer with the T790M mutation of epidermal growth factor receptor. Mol Cancer Ther 2010;9:1647-56.
11. Sos ML, Rode HB, Heynck S, Peifer M, Fischer F, Kluter S, et al. Chemogenomic profiling provides insights into the limited activity of irreversible EGFR Inhibitors in tumor cells expressing the T790M *EGFR* resistance mutation. Cancer Res 2010;70:868-74.
12. Meric-Bernstam F, Gonzalez-Angulo AM. Targeting the mTOR signaling network for cancer therapy. J Clin Oncol 2009;27:2278-87.
13. Zou ZQ, Zhang XH, Wang F, Shen QJ, Xu J, Zhang LN, et al. A novel dual PI3Kalpha/mTOR inhibitor PI-103 with high antitumor activity in non-small cell lung cancer cells. Int J Mol Med 2009;24:97-101.
14. Sheppard K, Kinross KM, Solomon B, Pearson RB, Phillips WA. Targeting PI3 kinase/AKT/mTOR signaling in cancer. Crit Rev Oncog 2012;17:69-95.
15. Mathew R, Karantza-Wadsworth V, White E. Role of autophagy in cancer. Nat Rev Cancer 2007;7:961-7.
16. Degenhardt K, Mathew R, Beaudoin B, Bray K, Anderson D, Chen G, et al. Autophagy promotes tumor cell survival and restricts necrosis, inflammation, and tumorigenesis. Cancer Cell 2006;10:51-64.
17. Amaravadi RK, Yu D, Lum JJ, Bui T, Christophorou MA, Evan GI, et al. Autophagy inhibition enhances therapy-induced apoptosis in a Myc-induced model of lymphoma. J Clin Invest 2007;117:326-36.
18. Amaravadi RK, Lippincott-Schwartz J, Yin XM, Weiss WA, Takebe N, Timmer W, et al. Principles and current strategies for targeting autophagy for cancer treatment. Clin Cancer Res 2011;17:654-66.
19. Svensson JP, Fry RC, Wang E, Somoza LA, Samson LD. Identification of novel human damage response proteins targeted through yeast orthology. PLoS One 2012;7:e37368.
20. Hou W, Han J, Lu C, Goldstein LA, Rabinowich H. Autophagic degradation of active caspase-8: a crosstalk mechanism between autophagy and apoptosis. Autophagy 2010;6:891-900.
21. Li X, Lu Y, Pan T, Fan Z. Roles of autophagy in cetuximab-mediated cancer therapy against EGFR. Autophagy 2010;6:1066-77.
22. Wu YT, Tan HL, Shui G, Bauvy C, Huang Q, Wenk MR, et al. Dual role of 3-methyladenine in modulation of autophagy via different temporal patterns of inhibition on class I and III phosphoinositide 3-kinase. J Biol Chem 2010;285:10850-61.
23. Powis G, Bonjouklian R, Berggren MM, Gallegos A, Abraham R, Ashendel C, et al. Wortmannin, a potent and selective inhibitor of phosphatidylinositol-3-kinase. Cancer Res 1994;54:2419-23.
24. Blommaart EF, Krause U, Schellens JP, Vreeling-Sindelarova H, Meijer AJ. The phosphatidylinositol 3-kinase inhibitors wortmannin and LY294002 inhibit autophagy in isolated rat hepatocytes. Eur J Biochem 1997;243:240-6.
25. Kaini RR, Hu CA. Synergistic killing effect of chloroquine and androgen deprivation in LNCaP cells. Biochem Biophys Res Commun 2012;425:150-6.
26. Rahim R, Strobl JS. Hydroxychloroquine, chloroquine, and all-trans retinoic acid regulate growth, survival, and histone acetylation in breast cancer cells. Anticancer Drugs 2009;20:736-45.
27. Klionsky DJ, Elazar Z, Seglen PO, Rubinsztein DC. Does bafilomycin A1 block the fusion of autophagosomes with lysosomes? Autophagy 2008;4:849-950.
28. Swampillai AL, Salomoni P, Short SC. The role of autophagy in clinical practice. Clin Oncol (R Coll Radiol) 2012;24:387-95.
29. Butaye P, Devriese LA, Haesebrouck F. Antimicrobial growth promoters used in animal feed: effects of less well known

antibiotics on gram-positive bacteria. Clin Microbiol Rev 2003;16:175-88.

30. Ketola K, Vainio P, Fey V, Kallioniemi O, Iljin K. Monensin is a potent inducer of oxidative stress and inhibitor of androgen signaling leading to apoptosis in prostate cancer cells. Mol Cancer Ther 2010;9:3175-85.